

NUMERICAL STUDY ON AGING DYNAMICS IN THE 3D ISING SPIN-GLASS MODEL — QUASI-EQUILIBRIUM BEHAVIOUR OF SPIN AUTO-CORRELATION FUNCTIONS

H. TAKAYAMA, H. YOSHINO and T. KOMORI*
*Institute for Solid State Physics, the University of Tokyo,
 Roppongi, Minato-ku, Tokyo 106-8666, Japan*

Received 1 September 1999
 Revised

Using Monte Carlo simulations, we have studied aging phenomena in three-dimensional Gaussian Ising spin-glass model focusing on quasi-equilibrium behavior of the spin auto-correlation functions. Weak violation of the time translational invariance in the quasi-equilibrium regime is analyzed in terms of effective stiffness for droplet excitations in the presence of domain walls. The simulated results in not only isothermal but also T -shift aging processes exhibit the expected scaling behavior with respect to the characteristic length scales associated with droplet excitations and domain walls in spite of the fact that the growth law for these length scales still shows a pre-asymptotic behavior compared with the asymptotic form proposed by the droplet theory. Implications of our simulational results are also discussed in relation to experimental observations.

Keywords: spin glass, aging, droplet theory

1. Introduction

In recent years aging dynamics in spin glasses has been extensively studied.^{1,2,3} A basic experimental protocol is isothermal aging process which is relaxation after the spin-glass system is quenched from temperature above the spin-glass temperature T_c to temperature T below T_c . One of the most interesting results in the simulational studies on 3D short-ranged Ising spin-glass model is that the coherence length $R_T(t)$ of the correlation function of real two replicas at time t after the quench grows in a power-law as,^{4,5,6} (but see also⁷)

$$R_T(t) \sim L_0(t/\tau_0)^{1/z}, \quad (1.1)$$

where L_0 is a certain characteristic length and exponent $1/z$ depends on T . The latter was obtained as $1/z(T) \simeq 0.17T$ for $T \leq 0.7$ in our previous paper⁶ which we refer to I hereafter. It is tempting to regard this $R_T(t)$ as a characteristic length of the ordering process, i.e., a mean distance of domain walls separating different

*Present address: Hydrographic Department, Maritime Safety Agency, 5-3-1 Tsukiji, Chuo-ku, Tokyo 104-0045, Japan.

pure states, which are parallel or anti-parallel to a ground state. In this respect, it is only the droplet theory,^{8,9} at the moment, that provides us some concrete scaling arguments based on such characteristic length scales as $R_T(t)$.

According to the droplet theory by Fisher and Huse (FH),⁹ isothermal aging in spin glasses is associated with coarsening of domain walls, which is driven by successive nucleation of thermally activated droplets. Up to waiting time t_w after the quench, domains of averaged size $R_T(t_w)$ have grown up. Within each domain small droplets of size L ($\ll R_T(t_w)$) are thermally fluctuating as they are almost in equilibrium: a typical value of their excitation gap F_L^{typ} scales as

$$F_L^{\text{typ}} \sim \Upsilon(L/L_0)^\theta, \quad (1.2)$$

where Υ is the stiffness constant, and that of free-energy barrier B_L^{typ} scales as

$$B_L^{\text{typ}} \sim \Delta(L/L_0)^\psi, \quad (1.3)$$

where Δ is a characteristic free-energy scale. The above two exponents satisfy $\theta \leq (d-1)/2$ and $\theta \leq \psi \leq d-1$ with d being dimension of the system.

However, there are some droplets which touch with the domain wall so that their excitation gap is reduced from eq.(1.2). This effect was studied by FH by making use of some geometrical and probabilistic arguments. Averaged over all droplets including those within the domain, FH has derived a typical value of excitation gaps of droplets with size L in the presence of the domain walls with mean separation R as

$$F_{L,R}^{\text{typ}} = \Upsilon^{\text{eff}}[L/R](L/L_0)^\theta, \quad (1.4)$$

with the effective stiffness constant given by

$$\Upsilon^{\text{eff}}[L/R] = \Upsilon \left(1 - c_v \left(\frac{L}{R} \right)^{d-\theta} \right), \quad (1.5)$$

where c_v is a numerical constant.

By making use of the above argument on the effective stiffness constant, the spin auto-correlation function

$$C_T(\tau; t_w) = \overline{C_{i,T}(\tau; t_w)} \quad \text{with} \quad C_{i,T}(\tau; t_w) = \langle S_i(\tau + t_w) S_i(t_w) \rangle_T, \quad (1.6)$$

is evaluated as the following. Some further details of its derivation are described in our separated paper¹⁰ which we refer to II hereafter. A droplet of size L enclosing spin S_i contributes to $C_{i,T}(\tau; t_w)$ as

$$C_{i,T}(\tau; t_w) \simeq \begin{cases} 1 & \text{for } \tau_L(i) > \tau, \\ < S_i >_T^2 \simeq 1 - 4\exp(-F_{L,R}(i)/T) & \text{for } \tau_L(i) < \tau, \end{cases} \quad (1.7)$$

where $\tau_L(i) = \tau_0 \exp(B_L(i)/T)$ is the relaxation time of the droplet whose free-energy barrier is $B_L(i)$. The averages (denoted by the over-line in eq.(1.6)) over

site i and different realizations of interactions (samples) are all taken into account by the probability distribution of free-energy gaps $F_{L,R}(i)$ which is assumed to scale as,

$$\rho_{L,R}(F) \simeq \frac{1}{F_{L,R}^{\text{typ}}} \tilde{\rho} \left(\frac{F}{F_{L,R}^{\text{typ}}} \right), \quad (1.8)$$

where a scaling function $\tilde{\rho}(x)$ satisfies $\tilde{\rho}(0) > 0$. Then, gathering the multiplicative contributions of droplets with various sizes, $L = 2^n L_0$; $n = 0, 1, 2, \dots$, enclosing spin S_i , we obtain

$$1 - C_T(\tau; t_w) \sim \int_{L_0}^{L_T(\tau)} \frac{dL}{L} \frac{\tilde{\rho}(0)T}{(L/L_0)^\theta} \frac{1}{\Upsilon^{\text{eff}}[L/R_T(t_w)]} \quad (1.9)$$

$$\sim 1 - C_{\text{eq},T}(\tau) + \frac{c_1 \tilde{\rho}(0)T}{\Upsilon(L_T(\tau)/L_0)^\theta} \left(\frac{L_T(\tau)}{R_T(t_w)} \right)^{d-\theta} + \dots, \quad (1.10)$$

where c_1 is a numerical constant and

$$1 - C_{\text{eq},T}(\tau) \sim \frac{T\tilde{\rho}(0)}{\Upsilon} \int_{L_0}^{L_T(\tau)} \frac{dL}{L} \frac{1}{(L/L_0)^\theta} = \frac{T\tilde{\rho}(0)}{\theta\Upsilon} \left[1 - \left(\frac{L_0}{L_T(\tau)} \right)^\theta \right]. \quad (1.11)$$

Here $R_T(t)$ is given by

$$R_T(t) \sim L_0[(T/\Delta)\ln(t/\tau_0)]^{1/\psi}. \quad (1.12)$$

and $L_T(\tau)$ by the same expression with t replaced by τ in accordance with eq.(1.3). The latter is the characteristic length of droplets which can fluctuate within time scale τ at temperature T . The above scaling expression eq.(1.10) is appropriate in the regime $L_T(\tau) \ll R_T(t_w)$ which defines the quasi-equilibrium regime of present interest. The third term in eq.(1.10) represents the leading correction to equilibrium behaviour which weakly violates the time translational invariance in this regime.

The simulational result eq.(1.1) differs from eq.(1.12). A possible interpretation of this discrepancy which we will pursue in the present work is as follow. The difference in the growth laws of $R_T(t)$ and $L_T(\tau)$ is simply due to two different time windows which one observes the aging processes; one is an asymptotic regime for which the droplet theory is constructed, and the other a pre-asymptotic regime that the simulations can observe. However, we consider that the scaling expressions written in terms of $R_T(t)$ and $L_T(\tau)$, such as eq.(1.10), are common to both regimes. A similar interpretation has been already proposed for some aspects of aging dynamics.^{7,11} In our paper II we have shown by detailed analysis on the spin auto-correlation function that the droplet picture in the sense described above in fact holds in the quasi-equilibrium of the isothermal aging in the 3D short-ranged Ising spin-glass model.

The main purpose of the present work is to demonstrate that the same picture consistently describes behavior of the aging dynamics in the *quasi-equilibrium*

regime of the so-called T -shift process.^{2,12} The latter is another typical experimental protocol of aging: first to let the system age isothermally at T_1 , to change temperature to T_2 at waiting time t_{w1} , to let the system age isothermally at T_2 in a period t_{w2} at which a small probing field is added, and then to measure response of the system at time τ afterwards. We may write the corresponding correlation function as $C_{T_2, T_1}(\tau; t_{w2}; t_{w1})$.

One of most interesting problems in the T -shift process is whether or how we can observe chaotic nature of the spin-glass phase which is derived from the droplet theory;^{8,13} namely, there exists such a characteristic length scale $L_{|T_1 - T_2|}$, called the overlap length, that the equilibrium spin-glass orders at T_1 and T_2 differ entirely from each other in the length-scale larger than $L_{|T_1 - T_2|}$. In the present work, as for the first step of our study on this problem, we have analyzed $C_{T_2, T_1}(\tau; t_{w2}; t_{w1})$ with $t_{w2} = 0$ in the *quasi-equilibrium regime* which is specified by $\tau \ll t_{w1}$. Up to now even a precursor of the chaotic nature has been ascertained within the time scale of our simulation. Instead, as mentioned above, the simulated results are consistently interpreted by the droplet picture without introduction of $L_{|T_1 - T_2|}$. In other words, $L_{|T_1 - T_2|}$, if it exists, is much larger than the length scale of our simulation.

After describing our model and numerical method in the next section, we briefly review the results on behaviors of the correlation function in the quasi-equilibrium regime of the isothermal aging in §3. We then present and discuss the corresponding results in the T -shift aging process in §4. In the last section we argue implications of our simulational results on the experimental observations based on the fluctuation-dissipation theorem.

2. Model and Method

We have carried out standard heat-bath Monte Carlo simulation on aging phenomena in the 3D Ising spin-glass model with Gaussian nearest-neighbor interactions with zero mean and variance $J = 1$. The spin-glass transition temperature is numerically determined most recently as $T_c = 0.95 \pm 0.04$.¹⁴ The data we will discuss below are obtained at $T = 0.5 \sim 0.8$ in $L_s = 24$ system averaged over 160 samples with one MC run for each sample. In our previous work,⁶ hereafter referred to I, it was confirmed that finite-size effects do not appear within our time window ($\lesssim 2 \times 10^5$ MCS) for these parameters. Also in I we showed from the finite-size-scaling analysis of relaxation of the energy per spin in isothermal aging that the exponent θ in eq.(1.2) at $T = 0.7, 0.8$ is estimated as $\theta = 0.20 \pm 0.03$ which coincides with the result of the defect energy analysis at $T = 0$.¹⁵

3. Results on Isothermal Aging

It is now well established that the correlation function $C_T(\tau; t_w)$ in isothermal aging consists of two characteristic time regimes, one is the range $\tau \ll t_w$ which is the quasi-equilibrium regime mentioned in §1, and the other $\tau \gg t_w$ called as

the out-of-equilibrium (or aging) regime. Our interest here is in its behaviors in the former regime. As shown in our paper II, characteristic features of $C_T(\tau; t_w)$ in the quasi-equilibrium regime are more easily understood when $1 - C_T(\tau; t_w)$ are analyzed as a function of t_w/τ with τ being fixed. It turns out that such data points of different τ lie top on each others when they are shifted vertically by proper amounts $\alpha_T(\tau)$. The results of such a one-parameter scaling are demonstrated in Fig. 1 where we plot

$$\Delta C_T(\tau; t_w) = 1 - C_T(\tau; t_w) - \alpha_T(\tau) \quad (3.1)$$

against t_w/τ . The $\{\alpha_T(\tau)\}$ thus determined are presented in the inset of Fig. 1 where we also show the results of the same analysis at different T 's. They appear as almost linear functions of $\ln\tau$.

In order to compare the above results with the scaling expressions eqs.(1.10) and (1.11), we only need to notice the fact that factor $(L_0/L_T(\tau))^\theta$ can be practically expanded as

$$\left(\frac{L_0}{L_T(\tau)}\right)^\theta = \left(\frac{\tau_0}{\tau}\right)^{\theta/z(T)} \simeq 1 - \frac{\theta}{z(T)} \ln\left(\frac{\tau}{\tau_0}\right), \quad (3.2)$$

since $\theta/z(T)$ is small as compared with $1/\ln(\tau_{\max}/\tau_0)$, where τ_{\max} ($= 512$) is the maximum τ in the present observation where we put $\tau_0 = 1$. Indeed, $\theta/z(T) \simeq 0.02$ with $\theta = 0.20 \pm 0.03$ and $1/z(T = 0.6) \simeq 0.102$, while $1/\ln(\tau_{\max}/\tau_0) \simeq 0.160$. This factor in eq.(1.10) can be approximated by its leading term ($= 1$), so that the last term in eq.(1.10) becomes a function of only $L_T(\tau)/R_T(t_w)$, which is given by

$$\Delta C_T(\tau; t_w) \propto (L_T(\tau)/R_T(t_w))^\kappa, \quad (3.3)$$

with $\kappa = d - \theta$. This is consistent with the fact that the one-parameter scaling shown in Fig. 1 does work well. The leading term of eq.(1.11), on the other hand, comes out from the second term in eq.(3.2), and we obtain

$$\alpha_T(\tau) = 1 - C_{\text{eq},T}(\tau) \simeq \frac{T\tilde{\rho}(0)}{\Upsilon} \frac{1}{z(T)} \ln\left(\frac{\tau}{\tau_0}\right). \quad (3.4)$$

This is quite consistent with nearly linear increase of $\alpha_T(\tau)$ shown in the inset of Fig. 1. Furthermore we obtain $\partial\alpha_T(\tau)/\partial\ln\tau \propto T^{2.4}$ from the data at four temperatures shown in the figure. This is compatible with eq.(3.4) which predicts the corresponding slope proportional to T^2 (note that $1/z(T) \propto T$). The extra T -dependence, which yields the power $T^{2.4}$ larger than T^2 , may be attributed to that of the factor $\tilde{\rho}(0)/\Upsilon$.

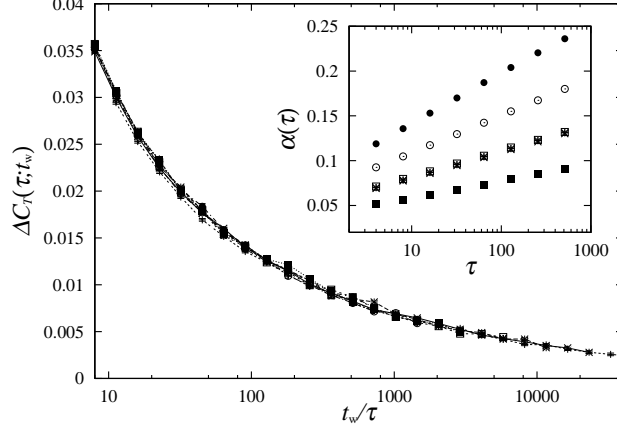


Fig. 1. The function $\Delta C_T(\tau; t_w)$ as a function of t_w/τ obtained in isothermal aging at $T = 0.6$. In the inset we show $\{\alpha(\tau)\}$ thus extracted at $T = 0.5, 0.6, 0.7$ and 0.8 from bottom to top. Four symbols at $T = 0.6$ represents four sets of $\{\alpha(\tau)\}$ which yield significantly different values of κ in eq.(3.3).

As for the determination of value κ in eq.(3.3), however, a more careful treatment is required since our simulational time window is not enough wide to extract precisely the limiting behavior of $\Delta C_T(\tau; t_w)$ at $L_T(\tau)/R_T(t_w) \rightarrow 0$. By the detailed analysis described in II, the values of κ acceptable within accuracy of the present simulated data are estimated as $\kappa \simeq 2.3 \sim 3.1$. The result is compatible with the expected value $d - \theta \simeq 2.8$, though the data of $\Delta C_T(\tau; t_w)$ alone cannot specify the value of θ . Let us remark also that this ambiguity in κ little affects the values of $\{\alpha_T(\tau)\}$, in particular, their slopes with respect to $\ln \tau$. This is demonstrated in the inset of Fig. 1 by drawing four sets of $\{\alpha_T(\tau)\}$ at $T = 0.6$ which yield $\kappa \simeq 2.2, 2.6, 3.0$, and 3.3 , respectively. These circumstances are similar at other temperatures we have examined. Therefore we show the representative results of $\{\alpha_T(\tau)\}$ in the inset of Fig. 1 which give rise to $\kappa \simeq 2.8 \sim 3.0$.

So far we have demonstrated that our simulated data of $C_T(\tau; t_w)$ are consistently interpreted by the scaling ansatz eq.(1.10), when the growth law of $R_T(t_w)$ eq.(1.12) in the droplet theory is replaced by eq.(1.1). We regard that the former describes the growth law in the asymptotic regime closer to equilibrium, while the latter does in the pre-asymptotic regime, and that the common scaling forms such as eq.(1.10) hold in both regimes.

4. Results on T -Shift Process

Among the T -shift aging processes described in §1, here we restrict ourselves to analysis on $C_{T_2, T_1}(\tau; t_{w2}; t_{w1})$ with $t_{w2} = 0$, which we abbreviate as $C_{T_2, T_1}(\tau; t_{w1})$. At time t_{w1} domains with mean separation $R_{T_1}(t_{w1})$ have grown up. It has been confirmed¹⁶ that, by the T -shift to T_2 at t_{w1} , the correlation length of the replica-

overlap function does not decrease. Rather it continues to increase though relatively gradually (rapidly) when $T_1 > (<) T_2$, and finally it merges to the isothermal curve $R_{T_2}(t)$ at T_2 at around $\tau = t_{w1}^{\text{eff}}$ which we define by the condition

$$R_{T_2}(t_{w1}^{\text{eff}}) \simeq R_{T_1}(t_{w1}), \quad \text{or} \quad t_{w1}^{\text{eff}} = a t_{w1}^{z(T_2)/z(T_1)}, \quad (4.1)$$

with a being a numerical constant rather close to unity. This means that $R_{T_1}(t_{w1})$ with t_{w1} we have examined does not exceed the overlap length $L_{|T_1-T_2|}$ mentioned in §1. That $L_{|T_1-T_2|}$, in case it exists, is much larger than the length scale of the presently available simulation agrees with the previous work.⁴ In the following, therefore, we analyze our data discarding the chaotic effect.

Then from the observed results mentioned above, we can simply think of a scenario that, in the time range $\tau \ll t_{w1}^{\text{eff}}$ after the T -shift, there exist domains nearly in equilibrium at T_1 and with mean separation of $R_{T_1}(t_{w1})$, and droplets up to mean size of $L_{T_2}(\tau)$ are fluctuating by thermal noises of temperature T_2 . In this situation with $R_{T_1}(t_{w1}) \gg L_{T_2}(\tau)$, which we call the *quasi-equilibrium regime* in the present T -shift aging process, $R_{T_1}(t_{w1})$ plays a role of $R_T(t_w)$ in equations which correspond to eqs.(1.10), (1.10) and (3.3). More explicitly, we expect that, if $1 - C_{T_2,T_1}(\tau; t_{w1})$ for various τ are plotted against t_{w1}^{eff}/τ , they look quite similar to the $1 - C_T(\tau; t_w)$ versus t_w/τ . Furthermore, as is the case for the latter shown in Fig. 1, $1 - C_{T_2,T_1}(\tau; t_{w1})$ are expected to lie on a universal curve by vertical shift, $\alpha_{T_2,T_1}(\tau)$, of the data for each τ . Indeed this is the case as shown in Fig. 2 where we plot

$$\Delta C_{T_2,T_1}(\tau; t_{w1}) = [1 - C_{T_2,T_1}(\tau; t_{w1})] - \alpha_{T_2,T_1}(\tau) \quad (4.2)$$

against t_{w1}^{eff}/τ .

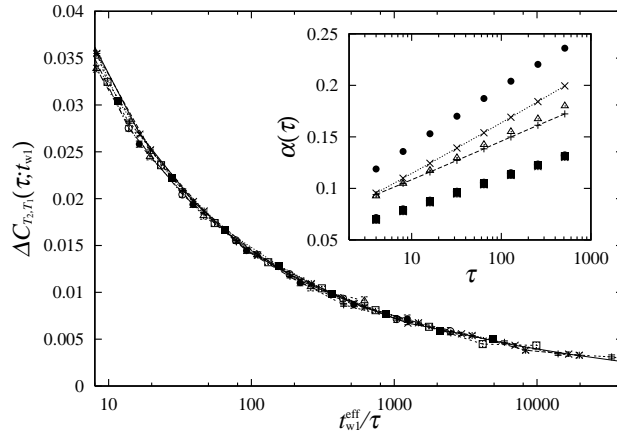


Fig. 2. The plot $\Delta C_{T_2,T_1}(\tau; t_{w1})$ versus t_{w1}^{eff}/τ for the T -shift process with $T_1 = 0.8$ and $T_2 = 0.6$. The functions $\alpha_{T_2,T_1}(\tau)$ thus extracted are presented in the inset: symbols with the dotted line represent $\alpha_{T_2=0.6,T_1=0.8}(\tau)$ and those with the broken line $\alpha_{T_2=0.8,T_1=0.6}(\tau)$, while only the symbols do the isothermal $\alpha_T(\tau)$ with $T = 0.6, 0.7$ and 0.8 from bottom to top.

The vertical shifts $\alpha_{T_2, T_1}(\tau)$ in eq.(4.2) depend on both T_1 and T_2 . To explain this let us go back to an equation for the local correlation function, which corresponds to eq.(1.7) for the isothermal process. In the present T -shift process deviation of the function from unity occurs also when a droplet enclosing spin S_i has relaxation time $\tau_L(i)$ which is smaller than τ , but the value it relaxes to is now given by

$$C_{i; T_1, T_2}(\tau; t_{w1}) \simeq \langle S_i \rangle_{T_1} \langle S_i \rangle_{T_2} \simeq 1 - 2[\exp(-F_{L,R}(i)/T_1) + \exp(-F_{L,R}(i)/T_2)], \quad (4.3)$$

for $\tau > \tau_L(i)$, since S_i here is regarded in equilibrium of temperatures T_1 and T_2 at times $\tau = 0$ and $\tau > \tau_L(i)$, respectively. Therefore we obtain, instead of eq.(3.4),

$$\alpha_{T_2, T_1}(\tau) \sim \frac{1}{2} \left(\frac{T_1 \tilde{\rho}(0)}{\Upsilon} + \frac{T_2 \tilde{\rho}(0)}{\Upsilon} \right) \frac{1}{z(T_2)} \ln \left(\frac{\tau}{\tau_0} \right). \quad (4.4)$$

This expression, combined with eq.(3.4), consistently explains the relative orders of slopes $\partial \alpha(\tau)/\partial \ln \tau$ ($= \Delta \alpha$) of various $\alpha(\tau)$ shown in the inset of Fig. 2; namely, $\Delta \alpha_{0.8} > \Delta \alpha_{0.8, 0.6} > \Delta \alpha_{0.7} > \Delta \alpha_{0.6, 0.8} > \Delta \alpha_{0.6}$.

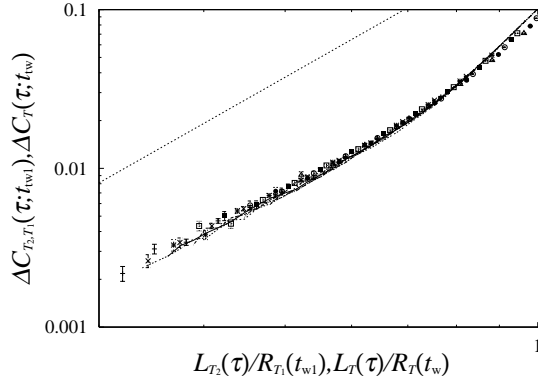


Fig. 3. The double logarithmic plot of $\Delta C_{T_2, T_1}(\tau; t_{w1})$ versus $L_{T_2}(\tau)/R_{T_1}(t_{w1})$ of the T -shift process for different τ 's are plotted by the different symbols (with $T_1 = 0.8$ and $T_2 = 0.6$). For comparison $\Delta C_T(\tau; t_w)$ versus $L_T(\tau)/R_T(t_w)$ of the isothermal aging for different τ 's are plotted by the different curves (at $T = 0.6$). The slope of the dotted line is 3.0.

Finally we show in Fig. 3 the double logarithmic plot of $\Delta C_{T_2, T_1}(\tau; t_{w1})$ versus $(\tau/t_{w1}^{\text{eff}})^{1/z(T_2)}$ which is proportional to $L_{T_2}(\tau)/R_{T_1}(t_{w1})$. For comparison, we also plot $\Delta C_T(\tau; t_w)$ versus $(\tau/t_w)^{1/z(T)}$ ($\propto L_T(\tau)/R_T(t_w)$) of the isothermal aging. Similarly to the latter case, there remains a relatively large ambiguity in the value of the slopes, i.e., the exponent which corresponds to κ in eq.(3.3). But the result is also compatible with $\kappa = d - \theta$ within accuracy of the present simulations.

5. Discussions

Our simulational results on the correlation function $C(t, t')$ ($= C_T(\tau; t_w)$ with $t = \tau + t_w$ and $t' = t_w$) so far described are closely related to the response function $G(t, t')$ via the fluctuation-dissipation theorem (FDT)

$$G(t, t') = \frac{1}{T} \frac{\partial C(t, t')}{\partial t'}, \quad (5.1)$$

and so the magnetic susceptibilities frequently measured in experiments. That the above FDT holds at least approximately in the quasi-equilibrium regime even with weak violation of the time-translational invariance (TTI) has been carefully checked experimentally.¹⁷ It has been also demonstrated in the simulational work by Franz and Rieger,¹⁸ though the authors did not mention it explicitly: their data which exhibit the FDT violate the TTI, i.e., depend also on t_w .

From eq.(5.1) the following relation between the out-of-phase component of the ac susceptibility $\chi_T''(\omega; t_w)$ and $C_T(\tau; t_w)$ in the isothermal aging is derived,

$$\chi_T''(\omega; t_w) \simeq -\frac{\pi}{2T} \frac{\partial}{\partial \ln \tau} C_T(\tau; t_w) \Big|_{\tau=\tau_\omega}, \quad (5.2)$$

where $\tau_\omega = 2\pi/\omega$. Its derivation and implication on the experimental results, such as the ωt_w -scaling of $\chi_T''(\omega; t_w)$, are described in II.

Here let us emphasize that from eq.(5.1) we obtain also the relation between $C(\tau; t_w)$ and the zero-field cooled susceptibility $\chi^{\text{ZFC}}(\tau; t_w)$ as

$$\chi^{\text{ZFC}}(\tau; t_w) = \int_{t_w}^{\tau+t_w} dt' G(\tau + t_w, t') = \frac{1}{T} [1 - C(\tau; t_w)]. \quad (5.3)$$

Thus $1 - C_T(\tau; t_w)$ in the isothermal aging, which we have analyzed in §3, is directly related to $\chi_T^{\text{ZFC}}(\tau; t_w)$ in the quasi-equilibrium regime. The similar relation is expected to hold in the *quasi-equilibrium regime* of the T -shift process which we have discussed in §4, i.e., when the response is examined by adding a probing field from $t_{w2} = 0$. Although $\chi_T^{\text{ZFC}}(\tau; t_w)$ has been measured frequently since the pioneering work by Lundgren *et al*¹⁹ and $\chi_{T_2, T_1}^{\text{ZFC}}(\tau; t_w)$ in the T -shift process with $t_{w2} = 0$ has been also examined,¹² most of the measurements have been focused on its crossover behaviour between the quasi-equilibrium and aging regimes. We believe that the detailed analyses on these $\chi^{\text{ZFC}}(\tau; t_w)$ are of quite importance since they will present us evidences for (or against) the droplet picture we have discussed in the present work.

To conclude, we have simulated aging dynamics in the 3D Ising spin-glass model, and analyzed behaviors of the spin auto-correlation function in the quasi-equilibrium regime of the T -shift aging processes. The simulated results, which are considered to represent aging properties in the pre-asymptotic regime, do not exhibit even a precursor of the chaotic nature of the spin-glass phase. Instead, they are satisfactorily explained by the scaling argument based on the characteristic length scales

$R_{T_1}(t_{w1})$ and $L_{T_2}(\tau)$, i.e., that of domains grown up till t_{w1} at T_1 and that of droplet excitations in time scales of τ at T_2 . However their growth law itself differs from the prediction by the droplet theory which is constructed for the asymptotic regime. We have conjectured that the experimental observation on $\chi^{\text{ZFC}}(\tau; t_w)$ in the quasi-equilibrium regime is of quite interest to check this droplet picture.

Acknowledgment

Two of the present authors (T. K. and H. Y.) were supported by Fellowships of Japan Society for the Promotion of Science for Japanese Junior Scientists. This work is supported by a Grant-in-Aid for International Scientific Research Program (#10044064) and by a Grant-in-Aid for Scientific Research Program (#10640362), from the Ministry of Education, Science and Culture. Most of the present simulation has been done on RANDOM at Material Design and Characterization Laboratory, Institute for Solid State Physics, University of Tokyo.

References

1. For a recent review see e.g. A. P. Young, *Spin-glasses and random fields* (World Scientific, Singapore, 1997).
2. E. Vincent, J. Hammann, M. Ocio, J.-P. Bouchaud and L.F. Cugliandolo, in *Proceeding of the Sitges Conference on Glassy Systems*, ed. E. Rubi, (Springer, Berlin, 1996) (preprint cond-mat/9607224.)
3. H. Rieger, in *Annual Review of Computational Physics II*, ed. D. Stauffer, (World Scientific, Singapore, 1995).
4. J. Kisker, L. Santen, M. Schreckenberg and H. Rieger, *Phys. Rev.* **B53** 6418 (1996).
5. E. Marinari, G. Parisi, F. Ricci-Tersenghi and J.J. Ruiz-Lorenzo, *J. Phys.* **A31** 2611 (1998).
6. T. Komori, H. Yoshino and H. Takayama, to appear in *J. Phys. Soc. Jpn.*, preprint cond-mat/9904143.
7. D.A. Huse: *Phys. Rev.* **B43** 8673 (1991).
8. D.S. Fisher and D.A. Huse, *Phys. Rev. Lett.* **56** 1601 (1986); A.J. Bray and M.A. Moore, in *Heidelberg Colloquium in Glassy Dynamics (Lecture Notes in Physics Vol. 275)*, ed. J.L. van Hemmen and I. Morgenstern, (Springer-Verlag, Heidelberg, 1987), p.121; D.S. Fisher and D.A. Huse, *Phys. Rev.* **B38** 386 (1988).
9. D.S. Fisher and D.A. Huse, *Phys. Rev.* **B38** 373 (1988).
10. T. Komori, H. Yoshino and H. Takayama, preprint cond-mat/9908078.
11. H. Rieger, *J. Phys.* **A26** L615 (1993).
12. P. Nordblad and P. Svendlidh, in Ref. 1, p.1.
13. A.J. Bray and M.A. Moore, *Phys. Rev. Lett.* **58** 57 (1987).
14. E. Marinari, G. Parisi and J.J. Ruiz-Lorenzo, *Phys. Rev.* **B58** 14852 (1998).
15. A.J. Bray and M.A. Moore, *J. Phys.* **C17** L463 (1984).
16. T. Komori, PhD Thesis, University of Tokyo, 1999.
17. M. Alba, J. Hammann, M. Ocio and Ph. Refregier, *J. Appl. Phys.* **61** 3683 (1987); Ph. Refregier, M. Ocio, J. Hammann and E. Vincent, *J. Appl. Phys.* **63** 4343 (1988).
18. S. Franz and H. Rieger, *J. Stat. Phys.* **79** 749 (1995).
19. L. Lundgren, P. Svendlidh, P. Nordblad and O. Beckman, *Phys. Rev. Lett.* **51** 911 (1983).